



Dopamine-dependent early synaptic and motor dysfunctions induced by α -synuclein in the nigrostriatal circuit

Alessandro Tozzi,^{1,†} Miriam Sciacaluga,^{1,†} Vittorio Loffredo,^{1,2} Alfredo Megaro,¹ Ada Ledonne,³ Antonella Cardinale,^{4,5} Mauro Federici,³ Laura Bellingacci,¹ Silvia Paciotti,¹  Elena Ferrari,⁶ Antonino La Rocca,² Alessandro Martini,³ Nicola B. Mercuri,^{3,7} Fabrizio Gardoni,⁶ Barbara Picconi,^{4,8} Veronica Ghiglieri,⁸ Elvira De Leonibus^{2,9} and Paolo Calabresi¹⁰

[†]These authors contributed equally to this work.

Misfolding and aggregation of α -synuclein are specific features of Parkinson's disease and other neurodegenerative diseases defined as synucleinopathies. Parkinson's disease progression has been correlated with the formation and extracellular release of α -synuclein aggregates, as well as with their spread from neuron to neuron. Therapeutic interventions in the initial stages of Parkinson's disease require a clear understanding of the mechanisms by which α -synuclein disrupts the physiological synaptic and plastic activity of the basal ganglia.

For this reason, we identified two early time points to clarify how the intrastriatal injection of α -synuclein-preformed fibrils in rodents via retrograde transmission induces time-dependent electrophysiological and behavioural alterations. We found that intrastriatal α -synuclein-preformed fibrils perturb the firing rate of dopaminergic neurons in the substantia nigra pars compacta, while the discharge of putative GABAergic cells of the substantia nigra pars reticulata is unchanged. The α -synuclein-induced dysregulation of nigrostriatal function also impairs, in a time-dependent manner, the two main forms of striatal synaptic plasticity, long-term potentiation and long-term depression. We also observed an increased glutamatergic transmission measured as an augmented frequency of spontaneous excitatory synaptic currents. These changes in neuronal function in the substantia nigra pars compacta and striatum were observed before overt neuronal death occurred.

In an additional set of experiments, we were able to rescue α -synuclein-induced alterations of motor function, striatal synaptic plasticity and increased spontaneous excitatory synaptic currents by subchronic treatment with L-DOPA, a precursor of dopamine widely used in the therapy of Parkinson's disease, clearly demonstrating that a dysfunctional dopamine system plays a critical role in the early phases of the disease. Although recent clinical trials targeting amyloid- β in Alzheimer's disease have shown promising results, there is increasing evidence suggesting that understanding alternative disease pathways that interact with amyloid- β metabolism and amyloid pathology might be important to halt the clinical deterioration. In particular, there is evidence supporting a critical role of astroglial activation and astrogliosis in Alzheimer's disease. However, so far, no studies have assessed whether astrogliosis is independently related to either amyloid- β or tau pathology *in vivo*.

To address this question, we determined the levels of the astrocytic marker GFAP in plasma and CSF of 217 amyloid- β -negative cognitively unimpaired individuals, 71 amyloid- β -positive cognitively unimpaired individuals, 78 amyloid- β -positive cognitively impaired individuals, 63 amyloid- β -negative cognitively impaired individuals and 75

Received January 02, 2021. Revised May 26, 2021. Accepted June 14, 2021. Advance access publication July 23, 2021

© The Author(s) (2021). Published by Oxford University Press on behalf of the Guarantors of Brain.

This is an Open Access article distributed under the terms of the Creative Commons Attribution-NonCommercial License (<https://creativecommons.org/licenses/by-nc/4.0/>), which permits non-commercial re-use, distribution, and reproduction in any medium, provided the original work is properly cited. For commercial re-use, please contact journals.permissions@oup.com

patients with a non-Alzheimer's disease neurodegenerative disorder from the Swedish BioFINDER-2 study. Participants underwent longitudinal amyloid- β (^{18}F -flutemetamol) and tau (^{18}F -RO948) PET as well as cognitive testing.

We found that plasma GFAP concentration was significantly increased in all amyloid- β -positive groups compared with participants without amyloid- β pathology ($P < 0.01$). In addition, there were significant associations between plasma GFAP with higher amyloid- β -PET signal in all amyloid- β -positive groups, but also in cognitively normal individuals with normal amyloid- β values ($P < 0.001$), which remained significant after controlling for tau-PET signal. Furthermore, plasma GFAP could predict amyloid- β -PET positivity with an area under the curve of 0.76, which was greater than the performance achieved by CSF GFAP (0.69) and other glial markers (CSF YKL-40: 0.64, soluble TREM2: 0.71). Although correlations were also observed between tau-PET and plasma GFAP, these were no longer significant after controlling for amyloid- β -PET. In contrast to plasma GFAP, CSF GFAP concentration was significantly increased in non-Alzheimer's disease patients compared to other groups ($P < 0.05$) and correlated with

amyloid- β -PET only in amyloid- β -positive cognitively impaired individuals ($P = 0.005$). Finally, plasma GFAP was associated with both longitudinal amyloid- β -PET and cognitive decline, and mediated the effect of amyloid- β -PET on tau-PET burden, suggesting that astrocytosis secondary to amyloid- β aggregation might promote tau accumulation.

Altogether, these findings indicate that plasma GFAP is an early marker associated with brain amyloid- β pathology but not tau aggregation, even in cognitively normal individuals with a normal amyloid- β status. This suggests that plasma GFAP should be incorporated in current hypothetical models of Alzheimer's disease pathogenesis and be used as a non-invasive and accessible tool to detect early astrocytosis secondary to amyloid- β pathology.

- 1 Department of Medicine and Surgery, University of Perugia, 06132 Perugia, Italy
- 2 Institute of Biochemistry and Cell Biology - IBBC, CNR, 00015 Monterotondo scalo, Italy
- 3 Laboratory of Experimental Neuroscience, Santa Lucia Foundation IRCCS, 00143 Rome, Italy
- 4 Department of Experimental Neurophysiology, IRCCS San Raffaele, 00166 Rome, Italy
- 5 Neurology, Department of Neuroscience, Faculty of Medicine, Università Cattolica del "Sacro Cuore", 00168 Rome, Italy
- 6 Department of Pharmacological and Biomolecular Sciences, University of Milan, 20133 Milan, Italy
- 7 Neurology Unit, Department of Systems Medicine, University of Rome "Tor Vergata", 00133 Rome, Italy
- 8 San Raffaele University, 00166 Rome, Italy
- 9 Telethon Institute of Genetics and Medicine, 80078 Pozzuoli, Italy
- 10 Neurological Clinic, Fondazione Policlinico Universitario Agostino Gemelli IRCCS, 00168 Rome, Italy

Keywords: long-term potentiation; long-term depression; Parkinson's disease; synaptic plasticity; substantia nigra

Abbreviations: DA = dopamine; EPSC = excitatory postsynaptic current; LTP = long-term potentiation; LTD = long-term depression; SPN = striatal projection neuron; SNpc/pr = substantia nigra pars compacta/pars reticulata; α -syn-PFF = α -synuclein-preformed fibrils; VTA = ventral tegmental area

Introduction

The two main pathological features of Parkinson's disease are represented by the progressive reduction of striatal dopamine (DA) innervation, originating from neurons located in the substantia nigra pars compacta (SNpc) and the presence of Lewy pathology, characterized by accumulations of α -synuclein (α -syn) proteinaceous fibrils.¹ Preclinical findings support the hypothesis that seeds of fibrillary α -syn, possibly originating from oligomeric forms, induce endogenous α -syn to aggregate in pathogenic inclusions.² Moreover, these aggregates can be released from neurons and spread throughout the brain.³

Experimental intrastriatal injection of α -syn-preformed fibrils (α -syn-PFF) in rodents induces Lewy-like pathology in dopaminergic neurons of the SNpc, followed by neuronal loss

and motor/behaviour features similar to Parkinson's disease.^{4–6} Several studies investigated the multiple mechanisms leading to α -syn-mediated degeneration and neuronal death in Parkinson's disease, such as impairment of lysosomal activity, mitochondrial dysfunction, altered endoplasmic reticulum-Golgi trafficking, abnormal calcium ion entry via the formation of pore-like structures, reduced protein degradation and increased oxidative stress.^{7,8}

The striatum represents the major basal ganglia nucleus, integrating inputs from the cortex and driving them to output stations of the basal ganglia; this nucleus plays a key role in the selection and chunking execution of action components.^{9,10} Striatal activity is also required to build motor patterns in response to sensory information and motivational experience.¹¹ In this nucleus, the

plasticity associated with goal-directed actions and motor learning involves glutamate release timed to local DA activity that, in turn, triggers the activation of intracellular cyclic adenosine monophosphate (cAMP)-dependent pathways in postsynaptic neurons.^{12,13} These pathways are involved in the regulation of striatal synaptic plasticity in physiological conditions¹² as well as in experimental Parkinson's disease¹⁴ and other movement disorders.¹⁵

Recently, we investigated the synaptic mechanisms through which initial motor learning is stored as long-term changes in striatal projection neurons (SPNs), and the specific role of nigrostriatal DA transmission in the establishment of this form of metaplasticity.¹⁶

A widespread dysfunction of striatal synaptic network can also be observed in both *in vitro* and *ex vivo* experiments in which α -syn, through modulation of specific N-methyl-D-aspartate (NMDA) receptor subunits, impairs long-term potentiation (LTP) in SPNs of the direct and indirect basal ganglia pathways.¹⁷ Notably, these early synaptic alterations are associated with visuospatial memory deficits but not with major loss of dopaminergic terminals or overt motor impairment.¹⁷

Based on this evidence, prevention of Parkinson's disease progression could possibly be achieved by targeting the formation and the extracellular release of α -syn aggregates, as well as their spreading from neuron to neuron throughout the nervous system.^{6,18–20} Therapeutic intervention in the early stage of Parkinson's disease also requires a clear understanding of the mechanisms by which α -syn disrupts the physiological synaptic and plastic activity of the basal ganglia, in particular of the nigrostriatal circuits, much earlier than an advanced degeneration of DA neurons. In this study, we identified two early time points to clarify how the intra-striatal injection of α -syn-PFF, by retrogradely affecting the SNpc, induces time-dependent motor and behavioural alterations by affecting the firing rate of DA SNpc neurons as well as distinct forms of corticostriatal plasticity such as LTP and long-term depression (LTD). Moreover, we investigated for the first time the role of the α -syn-dependent impairment of the dopaminergic nigrostriatal system in the initiation and progression of striatal synaptic properties and plasticity deficits related to motor dysfunctions.

Materials and methods

Animals

Adult male Wistar rats (Charles River Laboratories) weighing 250–275 g at the beginning of the experiments were used. Procedures on living animals were conducted in conformity with the European Directive 2010/63/EU in accordance with protocols approved by the Animal Care and Use Committee at the University of Perugia (Italy), IRCCS Fondazione Santa Lucia (Rome, Italy) and the Italian Ministry of Health. Rats were randomly assigned to the different experimental groups. The experimenters were blinded to the experimental groups when taking measurements.

Preparation of α -syn-PFFs

Lyophilized monomeric α -syn (recombinant human α -syn, Sigma-Aldrich) was dissolved in sterile PBS to a final concentration of 1 mg/ml ($\sim 70 \mu\text{M}$). α -Syn fibrils were assembled under constant shaking (600 rpm) at 37°C in benchtop tubes. Assembly reactions were placed in an orbital shaker (Eppendorf Thermomixer) for 7 days, and the aggregation process was monitored by thioflavin T assay. In particular, thioflavin T fluorescent dye (5 μM) was added to one replicate and the aggregation process was assessed by

reading the fluorescence at 480 nm in a CLARIOstar reader (BMG LABTECH). At the end of this procedure, α -syn PFF aliquots were stored at -80°C until used for intracerebral injection.¹⁷ Immediately before intracerebral injection, α -syn-PFF aliquots were thawed at room temperature and sonicated for a total of 60 pulses (0.5 s each for a total of 30 s) in an ultrasonic bath (Branson M2800H-E). Endotoxin levels were 0.0045 EU/ μg of protein (LAL endotoxin assay, Thermo Scientific).

Transmission electron microscopy

The samples of α -syn-PFF were examined with a transmission electron microscope (Talos L120C, Thermo Fisher) operating at 120 kV and digital images were acquired using a CETA-M™ 4 k × 4 k camera (Thermo Fisher).

Surgery

Seventy-two male Wistar rats were used. Surgical procedures were performed on deeply anaesthetized animals of 7–8 weeks of age [Zoletil®, 20 mg/kg plus xylazine 9 mg/kg, intraperitoneally (i.p.)]. Animals received two bilateral intra-striatal injections (1 μl at each site) of either 30 nM α -syn-PFF (1 mg/ml dissolved in PBS, $n = 43$) or PBS ($n = 29$). Stereotaxic striatal injections coordinates, taken with a tooth bar set at 0.00, were: (i) anteroposterior (AP) +1.0, mediolateral (ML) +3.0, dorsoventral (DV) -5.0 ; and (ii) AP +1.0, ML -3.0 , DV -5.0 .²¹ After surgery, the animals were monitored until awake and then returned to their cage. Some rats were used for behavioural tests and electrophysiology, others for behavioural tests and immunohistochemistry. Six or 12 weeks after surgery the animals were used for the experiments.

L-DOPA administration

α -Syn-PFF- and PBS-injected (sham) rats were treated with L-DOPA (6 mg/kg) plus benserazide (12 mg/kg) for 4 days (subchronic treatment i.p.) at 6 or 12 weeks after α -syn-PFF or PBS injection. The animals were used for behavioural tests, morphological characterization and electrophysiological measurements.

Behavioural tests

At 6 and 12 weeks after α -syn-PFF or PBS injection, animals were challenged with an inclined walking wire (grid) and open field tests. Each animal performed both tests once prior to sacrifice. Behavioural tests were carried out in the same room at the same time of day by an investigator blind to the state of the rat. The behaviour was scored using a video-tracking system (ANY-maze, Stoelting).

Inclined walking wire task

To analyse motor performance and reveal sensorimotor deficits in α -syn-PFF-injected rats, animals were forced to walk on an inclined grid. The task has been used to evaluate locomotor activity and coordination in rodent models of Parkinson's disease²² and was modified from a previous version.^{23,24} Achievement of the top edge of the grid, the end of the 5-min session or fall to the ground before the end of the 5-min session, set the end of the experiment.

Open field task

To assess the general locomotor activity level and exploratory behaviour, the animals were tested in the open field task for 10 min (600 s). Open field exploratory behaviour can also provide information on general level of anxiety-like behaviours by evaluating the

amount of time spent in the centre of the arena, which is generally anxiogenic for rodents.²⁵

Immunofluorescence

The rats were sacrificed following deep sedation. After sampling, the brains were stored in 4% paraformaldehyde (PFA) (Sigma Aldrich) at 4°C for at least 24 h and then passed in a PBS solution with 30% sucrose and 0.02% sodium azide and stored at 4°C for at least 24 h or until slicing. Slices (30 µm) were obtained using a cryostat (Leica CM1900) and stored in PBS with 0.02% sodium azide at 4°C for use in the histological procedures.

Striatal sections were incubated with the primary antibodies: rabbit phosphorylated α -syn (p- α -syn, phospho S129; ab51253, Abcam, 1:100) and tyrosine hydroxylase (TH, 1:1000, Millipore; MAB318) in PBS-containing bovine serum albumin (BSA, 0.1%) overnight at 4°C. Then, the sections were incubated for 2 h with the secondary antibodies Cy3 anti-rabbit (Jackson ImmunoResearch, 1:200) and Cy2 anti-mouse (Jackson ImmunoResearch, 1:200). Neuronal cells were counterstained with NeuroTrace™ 455 green fluorescent Nissl-stain. Striatal images were acquired using a Nikon confocal microscope (Nikon TiE2), with a 20× or 40× objective. Quantification of TH levels was performed on the ×20 images by densitometric analysis.

Slices of the substantia nigra were permeabilized with a PBS solution with 0.1% Triton™ X-100 (Sigma Aldrich) and 10% normal goat serum and blocked for 1 h with a PBS solution with 0.1% Triton™ X-100, 10% normal goat serum and 0.1% BSA. Primary antibodies of rat dopamine transporter (DAT) (1:500, MAB369; Merck Millipore) in combination with rabbit hu- α -syn phosphorylated at Ser129 (phospho S129-hu- α -syn, 1:100, ab51253, Abcam) and mouse TH (1:1000; MAB318; Merck Millipore) were applied overnight at 4°C. Slices were then incubated for 2 h at room temperature with the secondary antibodies: goat anti-rat fluorescein conjugated (1:300; AP136F, Merck Millipore), goat-anti rabbit Alexa Fluor® 568 (1:300; ab175470, Abcam) and goat anti-mouse Alexa Fluor® 488 (1:300; AP124J44, Merck Millipore). Slices of substantia nigra were stained with DAPI for nuclei visualization. Striatal images were acquired under a Nikon confocal microscope (Nikon TiE2), with a 20× or 40× objective. Quantification of TH levels was performed on ×20 images by densitometric analysis.

DAT/p- α -syn immunolabelling images were acquired by Hamamatsu NanoZoomer 2.0-RS slide scanner. TH immunolabelling images of the substantia nigra (×20 magnification) were acquired using a Leica DM6000B/M fluorescence upright microscope and Leica Application Suite (LAS-X) software.

Electrophysiology of the substantia nigra

Brain slicing

Acute midbrain slices from both PBS- and α -syn-PFF injected rats (6 and 12 weeks after surgery) were obtained following published procedures^{26,27} with minor changes. Rats were sacrificed and horizontal slices (250-µm thick) of the ventral midbrain containing the substantia nigra were cut using a vibratome (Leica VT1000S, Leica Microsystems). Slices were transferred to the recording chamber for the electrophysiological recordings, where they were continuously perfused at 2.5–3.0 ml/min with normal artificial CSF (33.0±0.5°C) containing: 126 mM NaCl, 24 mM NaHCO₃, 10 mM glucose, 2.5 mM KCl, 2.4 mM CaCl₂, 1.2 mM NaH₂PO₄ and 1.2 mM MgCl₂ saturated with 95% O₂–5% CO₂ (pH 7.4; ~290 mOsm).

Electrophysiology

Cell-attached and whole-cell patch-clamp recordings from DA neurons of SNpc and GABAergic neurons of substantia nigra pars reticulata (SNpr) were performed with glass borosilicate pipettes (4–7 MΩ) filled with a solution containing: 125 mM K-gluconate, 10 mM KCl, 10 mM HEPES, 2 mM MgCl₂, 4 mM ATP-Mg₂, 0.3 mM GTP-Na₃, 0.75 mM EGTA, 0.1 mM CaCl₂ and 10 mM phosphocreatine-Na₂ (pH 7.3 with KOH, ~280 mOsm).

The firing frequency was acquired for 5 min in the cell-attached configuration, before switching to the whole-cell configuration ($V_H = -60$ mV). Recordings were filtered at 1–4 kHz using the amplifier's in-built low-pass filter, digitized at 10 kHz and computer-saved. The mean frequency of spontaneous firing was measured during 2 min of recordings. To analyse neuronal excitability, a current-clamp configuration protocol consisting of 2 s-depolarizing current steps (+50/+200 pA, 50 pA step) was delivered to both SNpc DA and SNpr GABAergic neurons, while maintaining their membrane potential at $V_H = -60$ mV with current injection. The mean number of action potentials evoked by each current step was obtained by averaging the results from three stimulation protocols.

Electrophysiology of the nucleus striatum

Brain slicing

Rats were sacrificed by cervical dislocation and 220–240-µm thick corticostriatal coronal brain slices were prepared using a vibratome. Slices were maintained in Krebs solution, bubbled with a 95% O₂–5% CO₂ gas mixture at room temperature containing: 126 mM NaCl, 2.5 mM KCl, 1.2 mM MgCl₂, 1.2 mM NaH₂PO₄, 2.4 mM CaCl₂, 10 mM glucose and 25 mM NaHCO₃.¹⁷ Single slices were transferred to a recording chamber and submerged in a continuously flowing Krebs solution (34°C; 2.5–3 ml/min) bubbled with a 95% O₂–5% CO₂ gas mixture. Whole-cell patch-clamp recordings were performed from SPNs visualized using infrared differential interference contrast microscopy (Olympus) in the dorsal striatum.

Electrophysiological recordings

Whole-cell patch-clamp recordings (access resistance 15–30 MΩ; holding potential –80 mV) were performed with borosilicate pipettes (4–7 MΩ) filled with an internal solution containing: 145 mM K⁺-gluconate, 0.1 mM CaCl₂, 2 mM MgCl₂, 0.1 mM EGTA, 10 mM HEPES, 0.3 mM Na-GTP and 2 mM Mg-ATP adjusted to pH 7.3 with KOH.

A bipolar electrode, connected to a stimulation unit, was located in the white matter between the cortex and the striatum to stimulate glutamatergic fibres (0.1 Hz) and evoke excitatory postsynaptic currents (EPSCs), while the recording electrode was placed in the dorsolateral striatum. After recording evoked EPSCs of stable amplitudes for at least 10 min, a high frequency stimulation protocol, consisting of three trains of 3 s (20 s intervals), was delivered at 100 Hz to induce LTP or LTD. External Mg²⁺ ions were omitted from the solution to maximize the contribution of NMDA receptors during LTP experiments.¹⁷ In all patch-clamp experiments, 50 µM picrotoxin was added to the Krebs solution to block GABA_A receptors.

Constant potential amperometry

Amperometric detection of electrically-evoked DA release was performed in acute brain slices containing the dorsal striatum as described previously.^{28,29} Briefly, the DA-recording carbon fibre electrode was positioned near a bipolar Ni/Cr stimulating electrode, to a depth of 50–150 µm into the coronal slice. The imposed

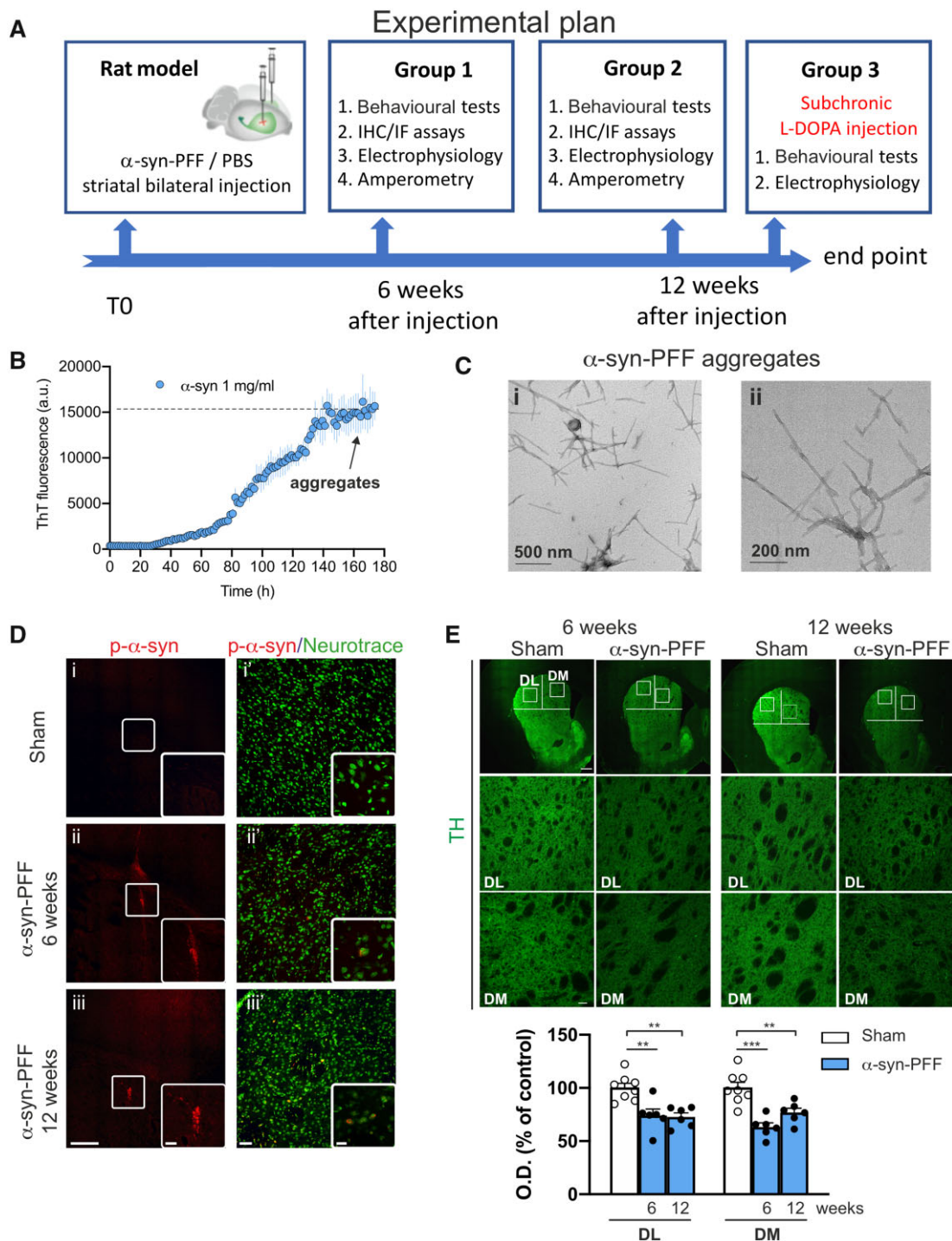


Figure 1 Graphical representation of the general experimental plan; procedure for aggregating α -syn and time-dependent immunofluorescence striatal characterization of the α -syn-PFF-injected rat model. (A) Scheme representing the timeline of the experimental procedures and the organization of the experimental groups. Rats were injected with α -syn-PFF or PBS at 7–8 weeks of age. After injection, the rats were enrolled in behavioural tests and then used for immunofluorescence (IF), electrophysiological or amperometric experiments. (B) Time-course graph of α -syn (1 mg/ml) aggregation in vitro, as increase in thioflavin T fluorescent staining. Note that after 160 h incubation, complete stable aggregates of α -syn (preformed fibrils, α -syn-PFF) are formed. (C) Transmission electron microscopy images showing α -syn-PFF at different magnifications before sonication. (D) Representative coronal brain images (i–iii) of p- α -syn immunofluorescence in the striatum of (i) sham (PBS-injected) and α -syn-PFF-injected rats at (ii) 6 weeks- and (iii) 12 weeks-post-injection, showing the site of α -syn-PFF injections (20 \times , scale bar = 500 μ m). The insets show higher magnification (digital zoom) of α -syn-positive aggregates (scale bar = 100 μ m). Representative images (i'–iii') of p- α -syn (red)/NeuroTrace™ 455 (green) double immunolabelling in striatum of (i') sham and α -syn-PFF-injected rats at (ii') 6 weeks- and (iii') 12 weeks-post-injection (20 \times objective, scale bar = 50 μ m). The insets show examples of higher magnification (40 \times with 2 \times digital zoom, scale bar = 20 μ m). (E) Representative images of coronal brain sections showing reduced TH immunoreactivity in the dorso-lateral (DL) and dorso-medial (DM) striatum of α -syn-PFF-injected rats (20 \times , scale bar = 500 μ m). The second and third row show the DL and DM striatal regions at higher magnification (\times 20, scale bar = 50 μ m) of the square areas outlined. The graph shows quantification of the TH immunoreactivity in the DL and DM striatum of sham- and α -syn-PFF-injected rats. Note the significant reduction of the TH staining both in the DL and DM striatum of 6- and 12-week-injected rats with respect to shams. Data are presented as mean \pm SEM of the optical density, as a percentage of the control. Sham n = 8; α -syn-PFF 6 weeks n = 6; α -syn-PFF 12 weeks n = 6; **P < 0.01, ***P < 0.001. One-way ANOVA, followed by Bonferroni's post hoc test.

voltage between the carbon fibre electrode and the Ag/AgCl pellet was 0.55 V. For stimulation, a single rectangular electrical pulse was applied every 5 min along a range of stimulation intensities (20–800 μ A, 20–70 μ s duration). In response to a protocol of increasing stimulation, a plateau of DA release was reached at maximal stimulation (800 μ A, 60 μ s).

Statistical analysis

The number of rats required was calculated in advance using G*Power3 software, setting power and confidence levels respectively to 80% and 95% and estimating the effect magnitude and standard deviation.

Behaviour

ANOVA followed by a *post hoc* test was performed. The number of experiments (*n*) represents the total number of animals tested for each experimental group.

Histology

TH, p- α -syn and DAPI immunoreactive neurons in the SNpc and in the ventral tegmental area (VTA) were counted manually by an experimenter blind to the treatment on 20 \times magnification images using ImageJ software (NIH, Bethesda, MD). For each experimental group, regularly spaced 30 μ m bilateral sections were chosen at multiple rostrocaudal levels to sample the SNpc and VTA. Specifically, we sampled considering the following anteroposterior coordinates relative to the bregma³⁰: -5.2 mm, -5.4 mm, -5.6 mm, -5.8 mm, -6.0 mm and -6.2 mm for the SNpc; -5.6 mm, -5.8 mm, -6.0 mm and -6.2 mm for the VTA. Sections from the sham and α -syn-PFF rats at 6 weeks post-injection and α -syn-PFF rats at 12 weeks post-injection were matched for each coordinate; cell numbers in the α -syn-PFF groups were expressed as the average percentage of cell numbers of the sham rats as previously reported.^{6,16}

Striatal TH immunoreactivity, expressed as optical density units, was measured in five square boxes (100 μ m per side) randomly positioned at different points on the image and considering background subtraction. Quantification was carried out in six regularly-spaced 30 μ m bilateral sections (corresponding approximately to the bregma: +1.8 mm, +1.56 mm, +1.32 mm, +1.08 mm, +0.84 mm and +0.60 mm). One-way ANOVA with treatment as the major factor was used.

Electrophysiology

Changes in the EPSC amplitude induced by drugs or by stimulation protocols were expressed as a percentage of the baseline, the latter representing the normalized EPSC mean amplitude acquired during a stable period (10–15 min) before delivering stimulation. In each experiment, the presence of LTP or LTD was verified using Student's *t*-test for paired samples by comparing the value of EPSC amplitude at the end of the recording (20–25 min) after the stimulation with that at the baseline. Statistical comparisons were performed using an unpaired Student's *t*-test, χ^2 test or one- or two-way ANOVA followed by a *post hoc* test as appropriate.

For the electrophysiological recordings, the number (*n*) of experiments represented the number of recorded neurons. Values in the text and figures are presented as mean \pm the standard error of the mean (SEM). Graphs represent the value of single experiments and mean \pm SEM. The significance level was established at $P < 0.05$.

Data availability

The data that support the findings of this study are available from the corresponding author upon reasonable request.

Results

α -Syn-PFFs were bilaterally injected in the dorsal striatum of adult male rats. The behavioural motor phenotype, striatal and nigral immunohistochemical analysis and electrophysiological recordings as well as striatal amperometric measures were then performed at 6 and 12 weeks post-injection (Fig. 1A). Stable α -syn-PFFs were prepared by *in vitro* aggregation of monomeric α -syn forms,¹⁷ confirmed by detection of thioflavin T fluorescence (Fig. 1B) and visualized by transmission electron microscopy (Fig. 1C).

α -Syn expression in the striatum and SNpc is paralleled by reduced TH+ cells in SNpc

The presence of α -syn in the dorsal striatum was confirmed by the presence of immunoreaction with the ser(129)-p- α -syn antibody at 6 and 12 weeks post-injection [Fig. 1D(ii and iii) and Supplementary Fig. 1]. PBS-injected sham rats did not present striatal p- α -syn immunoreactivity [Fig. 1D(i and i')]. We found that α -syn-PFF injection led to significant decrease in TH+ immunofluorescence in the dorso-lateral and dorso-medial striatum at both 6 and 12 weeks after PFF injection compared with PBS-injected rats (Fig. 1E).

We subsequently assessed whether α -syn could be carried retrogradely from the striatum to the SN and expressed in the SNpc of rats at 6 and 12 weeks post-injection. Thus, we performed DAT/p- α -syn double immunolabelling and observed a clear expression of pathological p- α -syn in SNpc dopaminergic neurons of α -syn-PFF-injected rats, sacrificed after 6 and 12 weeks, compared with neurons of PBS-injected sham rats (Fig. 2A). This finding suggests that, after striatal injection, α -syn-PFF can be retrogradely transported in the dopaminergic neurons of SNpc. Nigral dopaminergic neurons loss was subsequently evaluated by an immunolabelling count of TH+ cells both in the SNpc and VTA in PBS- and α -syn-PFF-injected rats. In the SNpc, a reduced, but not significant, dopaminergic cell number was found in α -syn-PFF rats 6 weeks after the injection, while a significant loss of neurons in rats 12 weeks after α -syn-PFF injection compared with the controls (Fig. 2B) was detected. Conversely, in the VTA of rats injected with α -syn-PFF, no differences were found in the counts of TH+ cells either at 6 or 12 weeks after α -syn-PFF injection compared with the controls (Fig. 2B). Interestingly, in the cortical regions of the slices used for striatal analysis, few p- α -syn positive neurons were found at the 6 week time point ($n = 5$), while a consistent proportion of positive neurons were detected at 12 weeks ($n = 5$). These neurons were localized mainly in layers IV and V of the cortex. Conversely, p- α -syn-positive neurons were absent in the sham-operated animals ($n = 5$) (Supplementary Fig. 2).

α -Syn-PFF injected rats show behavioural deficit in the grid-walking and open field tasks

To evaluate possible locomotor or motor coordination deficits in α -syn-PFF rats, we tested the animals in the grid-walking task. We found a significant increase in the latency to climb and immobility time in the 12-week group of α -syn-PFF rats but not in the 6-week group compared with the sham animals (Fig. 3A–C). No significant differences between groups were found in the latency to turn or mean speed, suggesting no coordination impairments (Supplementary Fig. 3).

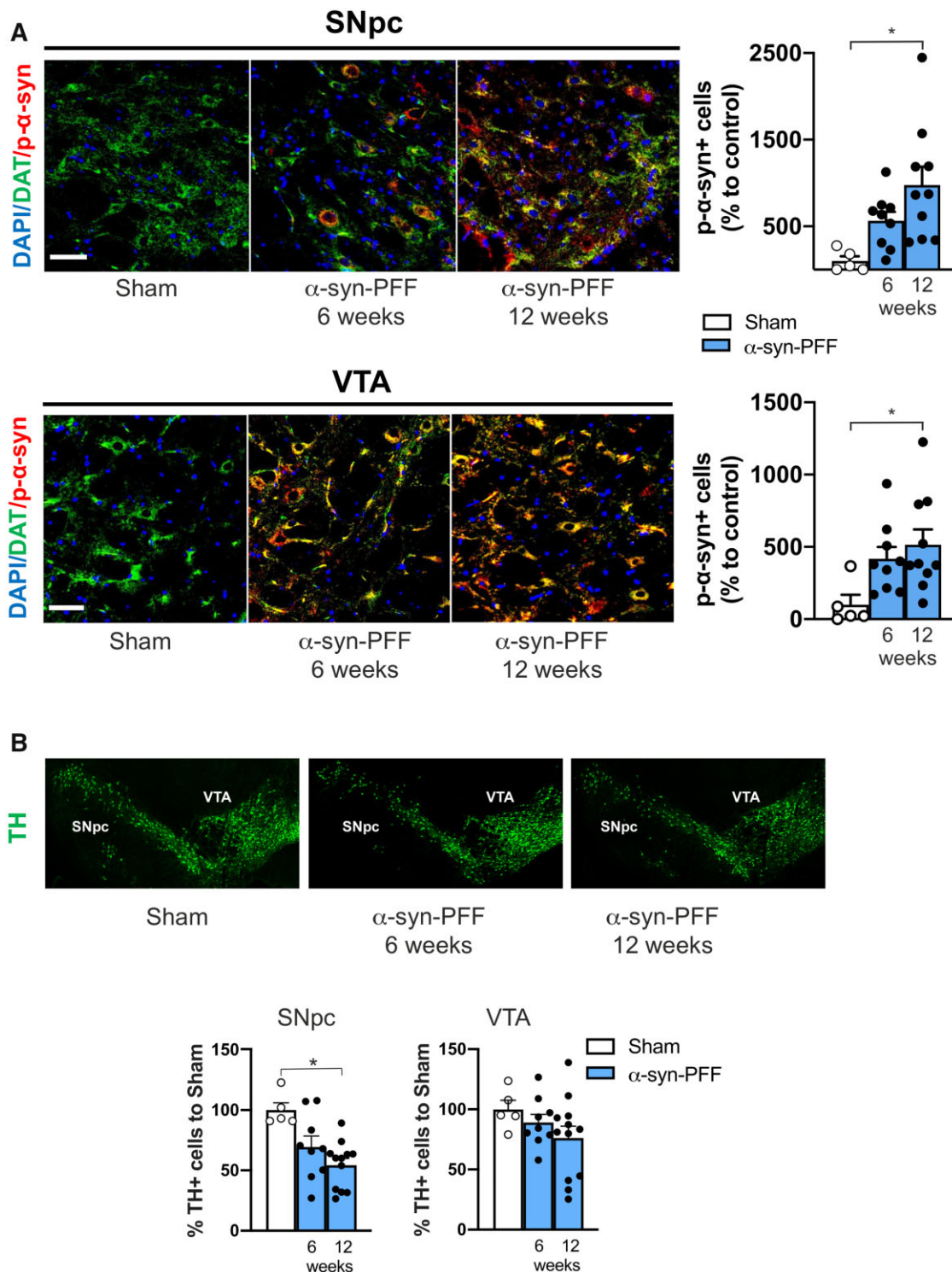


Figure 2 Striatal α -syn-PFF injection leads to a time-dependent increase of p- α -syn in the SNpc and VTA with parallel loss of SNpc TH-positive neurons. (A) Representative photomicrographs of SNpc (top) and VTA sections (bottom) of Sham- (left) and α -syn-PFF-injected rats, at 6 (middle) and 12 weeks after the injection (right), showing DAPI, DAT and p- α -syn triple co-immunofluorescence staining. Note that p- α -syn is mainly detected in dopaminergic neurons, as revealed by DAT immunostaining (20 \times magnification, 2 \times digital zoom, scale bar = 100 μ m). Graphs showing the counting of p- α -syn-positive cells of the SNpc (top) and VTA (bottom). Note the significant increase in the number of p- α -syn-positive neurons 12 weeks after α -syn-PFF injection compared with the sham (SNpc: sham n = 5; α -syn-PFF 6 weeks n = 9; α -syn-PFF 12 weeks n = 10. VTA: sham n = 5; α -syn-PFF 6 weeks n = 9; α -syn-PFF 12 weeks n = 10). (B) Representative photomicrographs sections, including the SNpc and VTA regions, of sham- (left) and α -syn-PFF-injected rats at 6 (middle) and 12 weeks (right) after injection, showing different degrees of TH immunofluorescence. Left graph shows the number of TH-positive neurons counted in the SNpc of α -syn-PFF-injected rats at 6 and 12 weeks post-injection (as a % of counts in shams). Note the significant reduction of TH-positive neurons in the SNpc of α -syn-PFF 12 weeks after the striatal injection (sham n = 5; α -syn-PFF 6 weeks n = 9; α -syn-PFF 12 weeks n = 12). The right graph shows the number of TH-positive neurons counted in the VTA of α -syn-PFF-injected rats at 6 and 12 weeks post-injection (as a % of counts in shams). Note that no significant differences between groups were found in the VTA (sham n = 5; α -syn-PFF 6 weeks n = 9; α -syn-PFF 12 weeks n = 12). *P < 0.05. One-way ANOVA followed by Bonferroni's post hoc test.

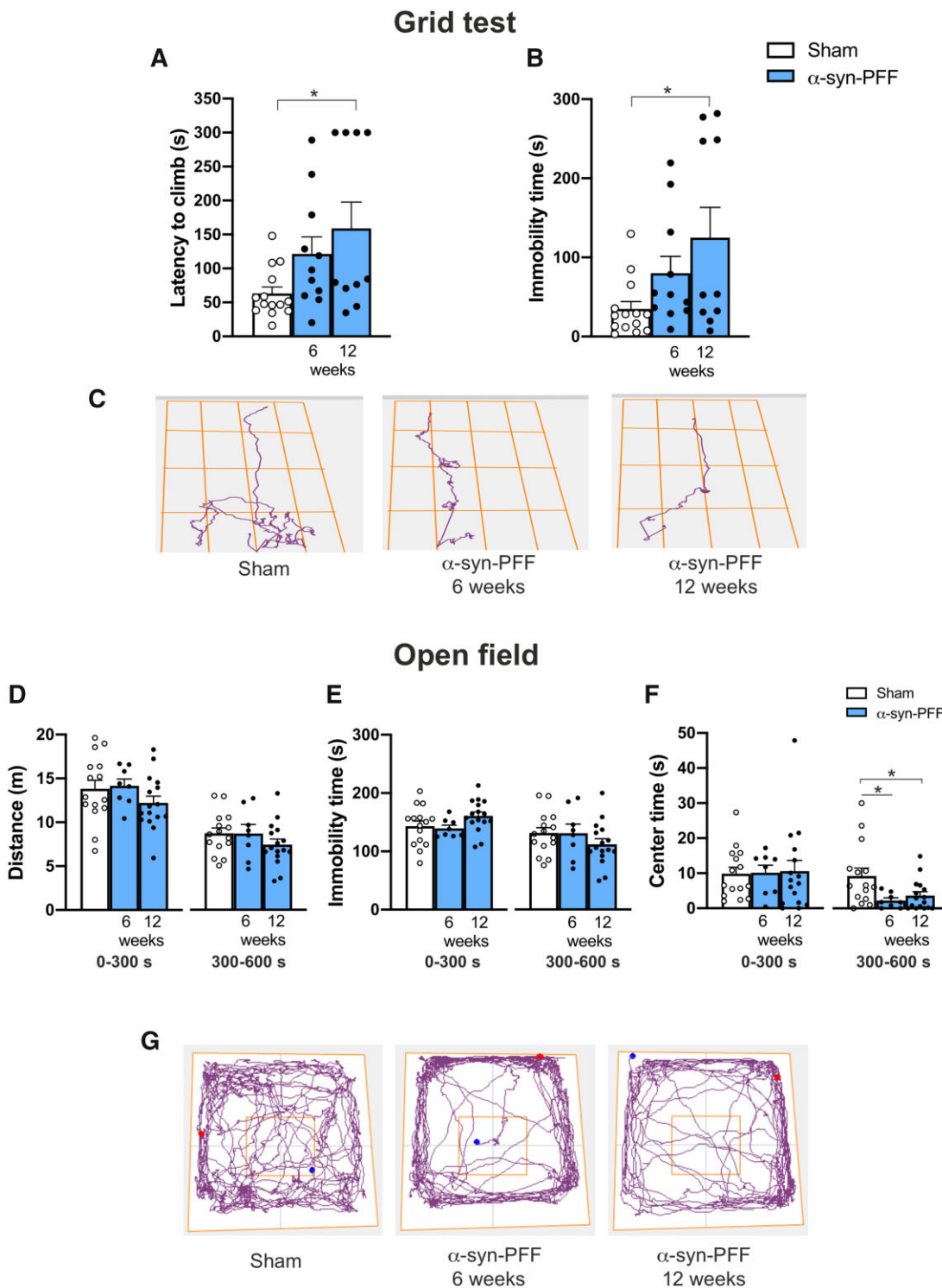


Figure 3 Intra-striatal α -syn-PFF injections lead to time-dependent onset of motor impairment in the grid-walking task and to early onset of anxiety-like behaviours. (A and B) Graphs of the performance of α -syn-PFF-injected rats in the grid-walking task showing increasing latency to climb (A) and immobility time (B) at 6 and 12 weeks after α -syn-PFF injection compared with sham rats; note that comparisons were significant 12 weeks after the injection (latency to climb and immobility time sham $n = 14$, α -syn-PFF 6 weeks $n = 11$; α -syn-PFF 12 weeks $n = 10$, $*P < 0.05$, mean \pm SEM. One-way ANOVA followed by Bonferroni's post hoc test). (C) Representative track plots of the route to the top of the grid for sham rats (left) and α -syn-PFF-injected rats 6 weeks (centre) and 12 weeks (right) post-injection. (D–F) Graphs of the distance travelled (D), immobility time (E) and time spent in the centre of the arena (F) of α -syn-PFF-injected and sham rats tested using the open field task. Note the reduced time spent in the centre of the arena for α -syn-PFF-injected rats with respect to Shams in the second part of the test (300–600 s), suggesting anxiety-like behaviour (sham $n = 15$, α -syn-PFF 6 weeks $n = 8$, α -syn-PFF 12 weeks $n = 16$) $*P < 0.05$, mean \pm SEM. One-way ANOVA followed by Bonferroni's post hoc test. (G) Representative track plots of rats performing the open field test. Note the reduced time spent in the centre of the arena of α -syn-PFF-injected rats at 6 and 12 weeks after the injection with respect to shams.

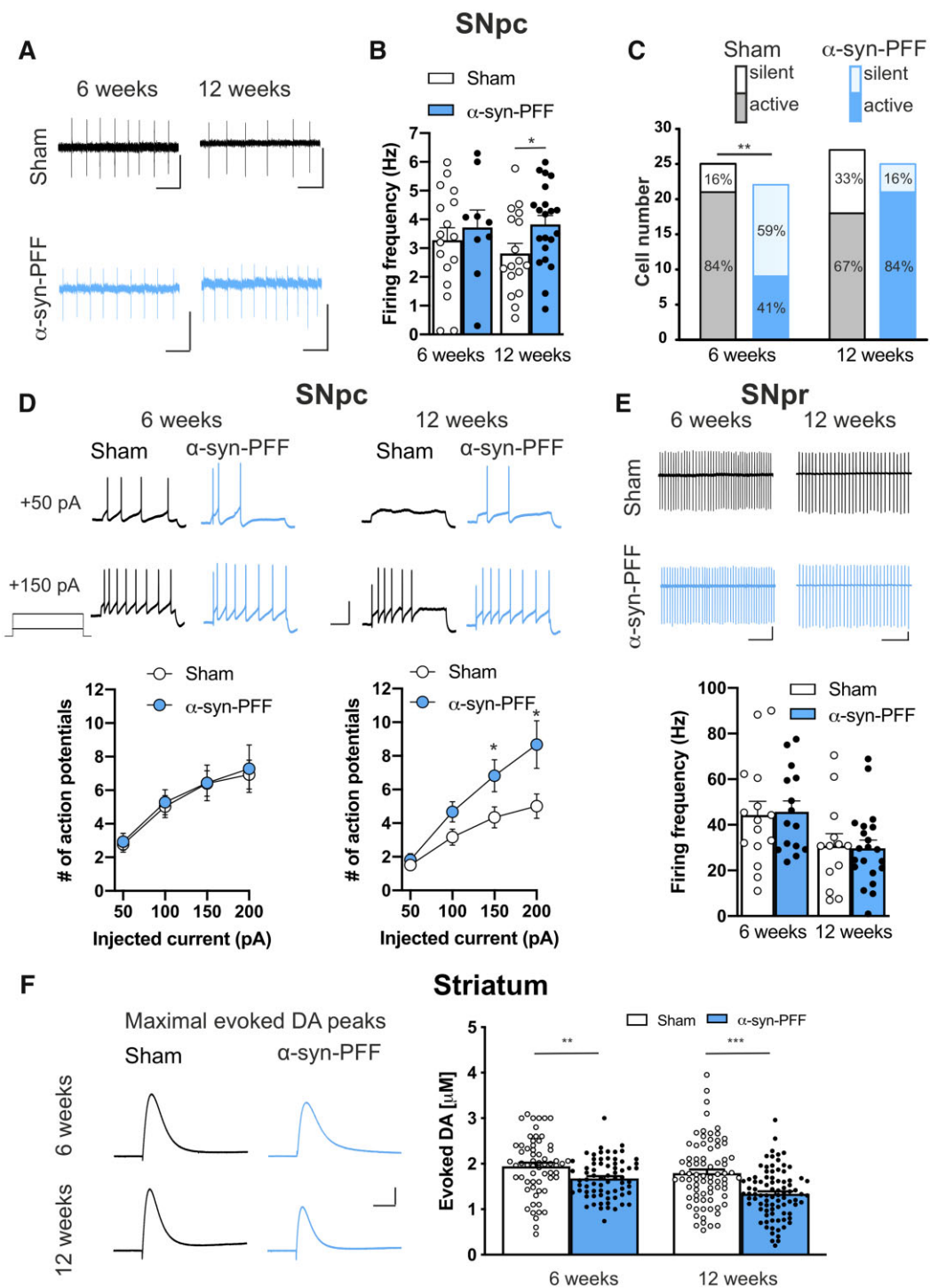


Figure 4 Electrical firing properties of nigral neurons and constant potential amperometry of striatal DA in slices of α -syn-PFF-injected and sham rats. (A) Representative traces of spontaneous firing recorded in cell-attached patch-clamp in DA neurons of SNpc in sham (black traces) and α -syn-PFF-injected (cyan traces) animals at 6 (left) or 12 weeks (right) after injection. Scale bars = 20 pA, 0.5 s. (B) Graph of the mean spontaneous firing frequency of active DA neurons in SNpc recorded from sham and α -syn-PFF rats at 6 and 12 weeks post-injection, showing a significant increase in the mean frequency in neurons of 12 weeks α -syn-PFF-injected rats respect to the sham animals (6 weeks: sham $n = 17$, α -syn-PFF $n = 9$; 12 weeks: sham $n = 17$, α -syn-PFF $n = 21$). Values are expressed as mean \pm SEM, * $P < 0.05$, Student's t -test. (C) Bar graph showing the number of recorded DA cells and the percentage of silent versus active neurons in the SNpc of sham (grey) and α -syn-PFF-injected (cyan) rats at 6 or 12 weeks post-surgery (active cells: 6 weeks, sham 21/25, α -syn-PFF 9/22; 12 weeks, sham 18/27, α -syn-PFF 21/25, ** $P = 0.002$, χ^2 test). (D) Representative traces of action potentials discharge in response to +50 and +150 pA current steps (top) and graphs of the number of action potentials (bottom) of SNpc DA neurons of sham and α -syn-PFF rats at 6 or 12 weeks after injection. Data are expressed as mean \pm SEM, * $P < 0.05$, Student's t -test. Scale bars = 40 mV, 0.5 s. (E) Representative traces of spontaneous firing recorded in GABAergic neurons of SNpr in sham (black traces) and α -syn-PFF (cyan traces) animals at 6 or 12 weeks post-injection. Scale bars = 25 pA, 250 ms. Graph of the mean spontaneous firing frequency of GABAergic neurons of the SNpr showing no differences between sham and α -syn-PFF rats at both 6 and 12 weeks post-injection (6 weeks: sham $n = 15$, α -syn-PFF $n = 15$; 12 weeks: sham $n = 13$, α -syn-PFF $n = 21$). (F) Representative traces (left) and graph (right) of constant potential amperometry of electrically-stimulated DA release performed in slices containing the dorsal striatum of sham and α -syn-PFF animals at 6 or 12 weeks after injection (6 weeks: sham $n = 62$, α -syn-PFF $n = 70$; 12 weeks: sham $n = 77$, α -syn-PFF $n = 87$). Data are expressed as mean \pm SEM, ** $P < 0.01$; *** $P < 0.001$, Student's t -test. Scale bars = 50 pA, 0.2 s.

To evaluate general locomotor performance and anxiety-like behaviour, 6- and 12-week α -syn-PFF- and PBS-injected rats were subjected to the open field task (Fig. 3D–G). Statistical comparisons between this control and both the 6- and 12-week α -syn-PFF groups showed no differences in the distance travelled and immobility time for both the first 5 min (0–300 s) and following 5 min (300–600 s) (Fig. 3D, E and G). However, we found that 6- and 12-week PFF- α -syn rats spent less time in the centre of the arena compared with the sham animals (Fig. 3F and G). Data collected in the open field apparatus suggested that striatal α -syn-PFF injection in rats led to early onset of reduced exploration, possibly revealing anxiety-like behaviour. However, α -syn-PFF rats showed no motor impairments in this task with respect to observations during the grid-walking task, suggesting a different sensitivity of the two tests in detecting mild motor dysfunctions.

α -Syn-PFF injected rats show altered firing activity of SNpc dopaminergic neurons and reduced striatal dopamine release

To explore whether α -syn-PFF injection might influence basal ganglia neuronal physiology, we first investigated the possible effects of α -syn-PFF on substantia nigra neurons. Dopaminergic neurons of the SNpc presented no alterations of the typical H-currents in both α -syn-PFF-injected and sham rats either at 6 or 12 weeks post-injection (Supplementary Fig. 4). Both groups also responded to acute exogenous application of DA producing outward currents of similar amplitudes and kinetics, as measured using whole-cell patch-clamp experiments (Supplementary Fig. 5). Conversely, we found that DA neurons of α -syn-PFF rats presented increased spontaneous firing frequency, with respect to neurons of sham rats, at 12 weeks but not at 6 weeks post-injection (Fig. 4A and B). Interestingly, we found that α -syn-PFFs affected the number of recorded neurons that presented spontaneous firing activity. In fact, the presence of active DA neurons was significantly reduced in the SNpc of α -syn-PFF rats at 6 weeks but not at 12 weeks after α -syn-PFF injection (Fig. 4C). The analysis of the current-voltage relationship also revealed a difference in the number of action potentials evoked by depolarizing steps of currents. In fact, statistical analysis showed that α -syn-PFF rats at 12 weeks post-injection presented a higher number of evoked action potentials of DA neurons with respect to those of sham rats, whereas this difference was absent between α -syn-PFF and sham rats at 6 weeks post-injection (Fig. 4D). While these findings revealed changes in the firing activities of SNpc DA neurons, we found that SNpr neurons showed no difference in the spontaneous firing frequency, suggesting that this region might be less affected by α -syn-PFF at both 6- and 12-weeks after injection (Fig. 4E).

Changes in the DA neurons firing activity might reflect abnormal striatal DA release.³¹ Constant potential amperometry experiments were designed to measure the synaptic release of DA by SNpc terminals in the striatum. Repetitive electrical stimulation of striatal slices evoked DA peaks in slices of α -syn-PFF rats that were significantly smaller than those evoked in slices of sham animals at both 6 and 12 weeks post-injection (Fig. 4F), suggesting that the alteration of nigral neurons is able to significantly influence striatal neuronal function and physiology.

α -Syn-PFF injection affects bidirectional synaptic plasticity of striatal spiny projection neurons

To explore the possible effects of α -syn-PFF injection on striatal function, we conducted patch-clamp recordings of striatal SPNs of α -syn-PFF and sham rats at 6 and 12 weeks post α -syn-PFF injection. We found that basal electrical properties of neurons were

unaltered at both time points, as shown by the analysis of the current-voltage curves and evoked firing activity (Supplementary Fig. 6). Moreover, the analysis of spontaneous synaptic currents showed increased spontaneous EPSC (sEPSC) frequency but not amplitude in SPNs of α -syn-PFF-injected rats 12 weeks post-injection with respect to the sham animals, whereas no differences were detected at 6 weeks after the α -syn-PFF injection (Fig. 6E and Supplementary Fig. 7). Interestingly, we discovered profound alterations to SPN long-term synaptic plasticity (Fig. 5). We found that at 6 weeks after α -syn-PFF or PBS injection, while the SPN LTD of α -syn-PFF rats was normal and similar to that of sham animals, it was significantly and strongly reduced at 12 weeks after the α -syn-PFF injection compared with the sham animals (Fig. 5A and B) and naïve untreated rats (Supplementary Fig. 8). SPN LTP was also profoundly impaired by α -syn-PFF, since it was absent in SPNs of α -syn-PFF-injected rats at both 6 and at 12 weeks after PFF injection (Fig. 5C, D and Supplementary Fig. 8).

L-DOPA subchronic treatment of α -syn-PFF-injected rats improves motor performance and reverses the altered SPN electrophysiological changes

In the attempt to counteract the functional and behavioural alterations found in α -syn-PFF rats, we treated α -syn-PFF and sham animals with subchronic injections of 6 mg/kg L-DOPA i.p. for 4 days. The rats were subsequently tested in the grid-walking task and afterwards were sacrificed to perform electrophysiological recordings of striatal SPNs. We found that at 12 weeks post-surgery, while rats injected with α -syn-PFF that were naïve to L-DOPA presented significantly increased latency to climb and immobility time with respect to sham, α -syn-PFF animals treated with L-DOPA showed no difference compared with the sham animals (Fig. 6A and B); this suggested that subchronic L-DOPA treatment was able to normalize the motor behaviour defects caused by α -syn-PFF 12 weeks after the injection. Interestingly, L-DOPA treatments also fully reversed the synaptic activity and plasticity deficits of striatal SPNs produced by α -syn-PFF 12 weeks after injection. In fact, α -syn-PFF rats treated with L-DOPA presented a normal LTD (Fig. 6C) and a full LTP expression (Fig. 6D) of striatal SPNs compared with L-DOPA-treated sham animals. L-DOPA also normalized SPN spontaneous excitatory synaptic currents, since no differences were found in the sEPSC amplitude or frequency in SPNs of L-DOPA-treated α -syn-PFF and sham rats. However, in rats that were naïve to L-DOPA, α -syn-PFF-injection significantly increased the sEPSC frequency (Fig. 6E and Supplementary Fig. 7). We found that the effect of L-DOPA subchronic treatment was dependent on the time from α -syn-PFF injection. In fact, at 6 weeks post- α -syn-PFF-injection, the rats presenting an increasing trend in performance in the grid walking task showed a mild amelioration of the motor performance with L-DOPA treatment (Supplementary Fig. 9A). Moreover, at 6 weeks after α -syn-PFF or PBS injection, SPNs of α -syn-PFF-injected rats that were subchronically treated with L-DOPA showed a small unstable synaptic potentiation that was significantly different from a full LTP (Supplementary Fig. 9B). Taken together, these findings were suggestive of a time-dependent restorative effect of subchronic L-DOPA treatment on motor behaviour and striatal synaptic transmission and plasticity.

Discussion

The aggregation of α -syn causes dysfunction and degeneration of multiple classes of neurons in Parkinson's disease.³ Mutations in the SNCA gene, which encodes α -syn, cause familial forms of Parkinson's disease, but this protein seems to be also involved in sporadic Parkinson's disease pathophysiology.³² The critical role of

Striatal SPNs

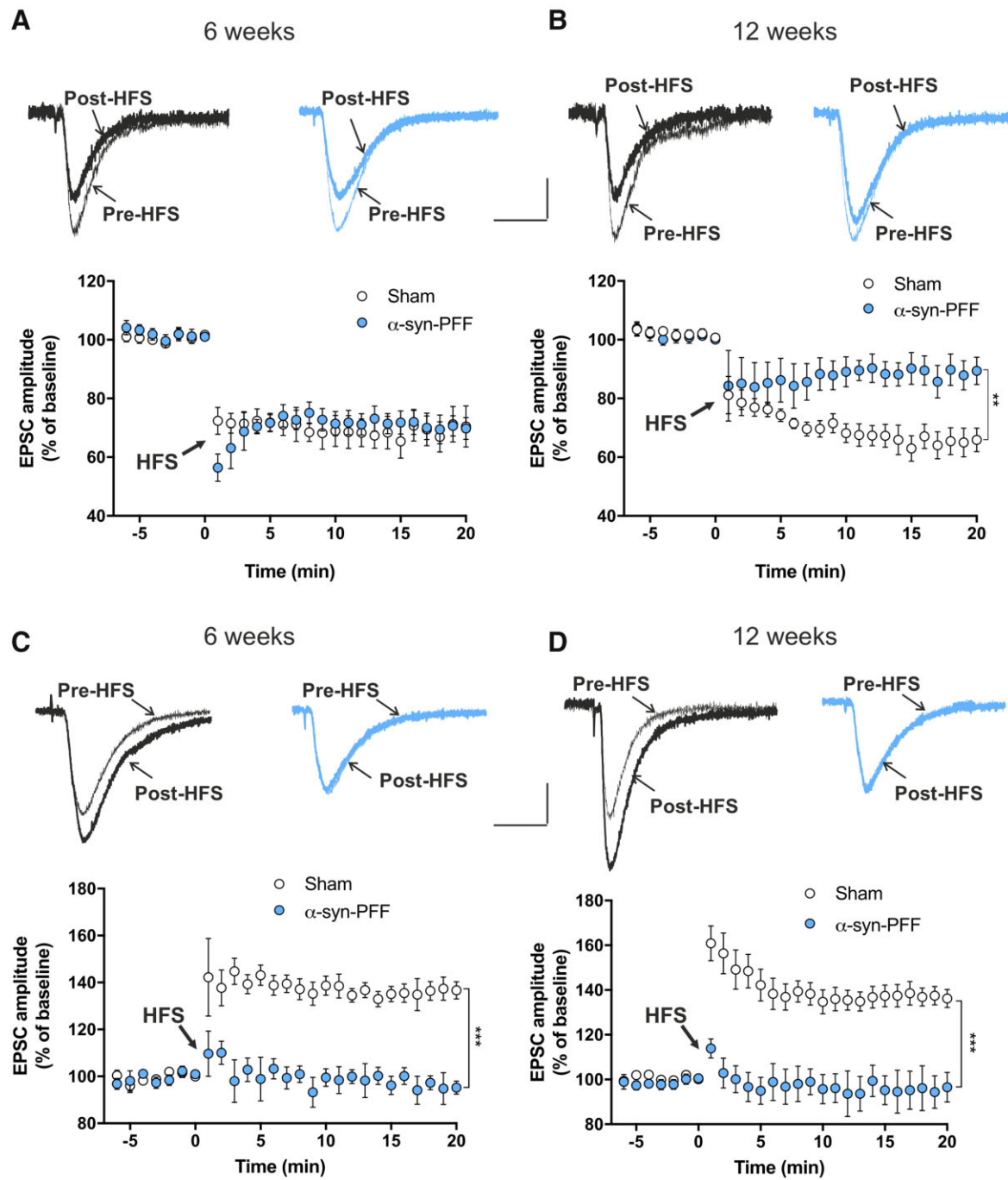


Figure 5 Time course of LTD and LTP of striatal spiny projection neurons of α -syn-PFF- and PBS-injected rats at 6 and 12 weeks post-injection. (A and B) Representative traces of superimposed evoked EPSCs recorded from a SPN before and 20 min after a high-frequency stimulation (HFS) protocol in sham (black traces) and α -syn-PFF-injected (cyan traces) animals at 6 weeks (A, top) or 12 weeks (B, top) from injection. The time-course graphs show the mean EPSC amplitudes, as a percentage of the baseline, of SPNs recorded before and for 20 min after an HFS (LTD protocol) in both sham and α -syn-PFF rats at 6 weeks (A) and 12 weeks (B) post-surgery. Note the reduced LTD in α -syn-PFF rats at 12 weeks post-injection (6 weeks: sham $n = 6$, α -syn-PFF $n = 7$; 12 weeks: sham $n = 8$, α -syn-PFF $n = 9$), $**P < 0.01$, two-way ANOVA. (C and D) Representative traces of superimposed evoked EPSCs recorded from a SPN in a Mg^{2+} -free Krebs solution before and 20 min after an HFS protocol, in sham (black traces) and α -syn-PFF (cyan traces) animals at 6 weeks (C, top) or 12 weeks (D, top) from injection. The time-course graphs show the mean EPSC amplitudes, as a percentage of the baseline, of SPNs recorded before and for 20 min after the HFS (LTP protocol) in both sham and α -syn-PFF rats at 6 weeks (C) and 12 weeks (D) post-surgery. Note the absence of LTP in SPNs of α -syn-PFF rats at both 6 and 12 weeks post-surgery (6 weeks: sham $n = 9$; α -syn-PFF $n = 13$; 12 weeks: sham $n = 9$; α -syn-PFF $n = 9$), $***P < 0.001$, two-way ANOVA. Scale bars = 100 pA, 20 ms.

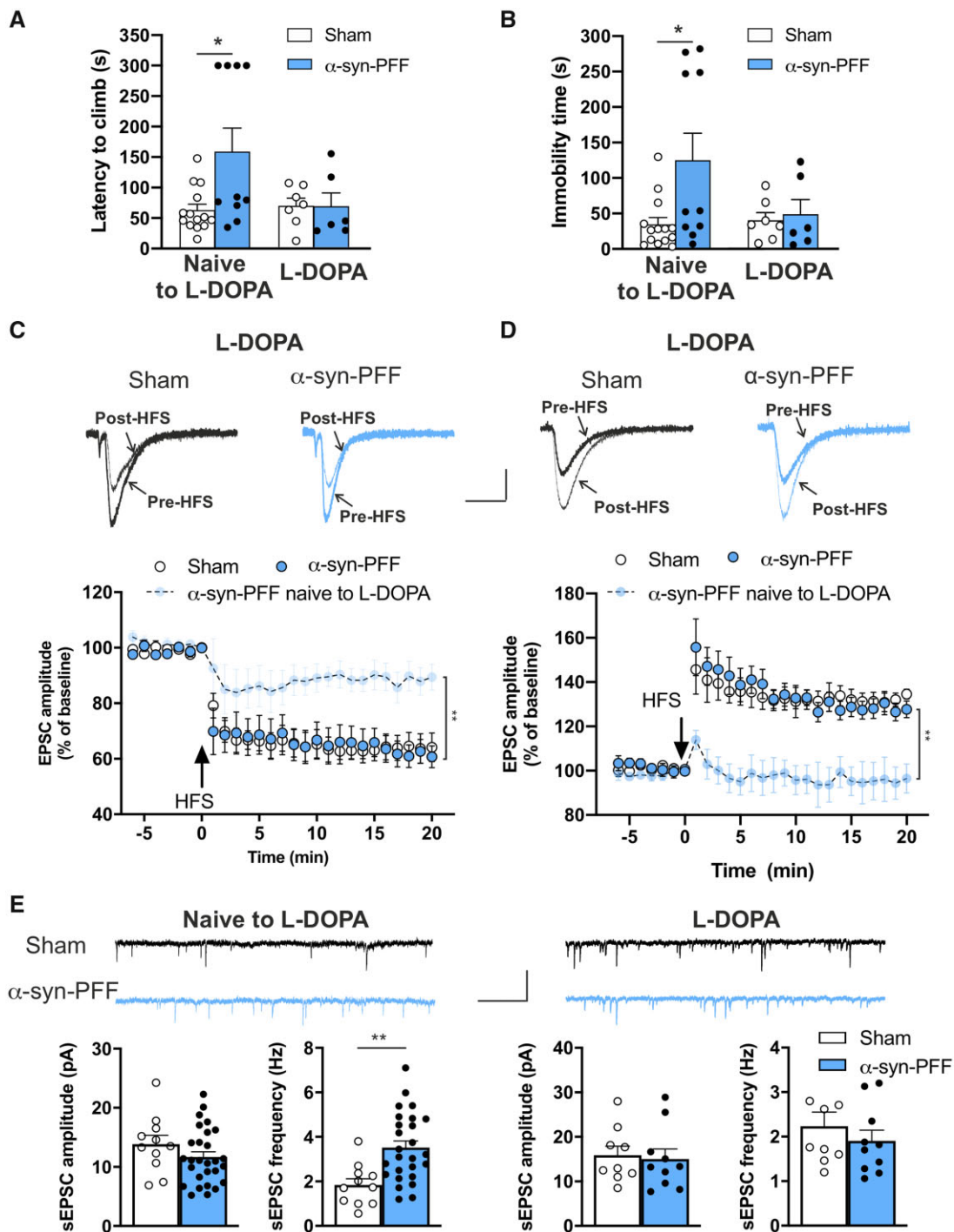


Figure 6 Effect of subchronic L-DOPA treatment on synaptic spontaneous currents, synaptic plasticity and motor performance of rats at 12 weeks post α -syn-PFF- or PBS-injection. (A and B) Graphs of the performance of α -syn-PFF- and PBS-injected rats treated with L-DOPA in the grid-walking task show that the latency to climb (A) and the immobility time (B) at 12 weeks after α -syn-PFF injection are not significantly different, unlike the observations of α -syn-PFF and sham rats that were naïve to L-DOPA (naïve to L-DOPA: sham $n = 14$, α -syn-PFF $n = 10$, $*P < 0.05$; L-DOPA: sham $n = 7$, α -syn-PFF $n = 6$, one-way ANOVA followed by Bonferroni's *post hoc* test). (C) Representative superimposed evoked EPSCs recorded from a SPN before and 20 min after a high-frequency stimulation (HFS) protocol in sham (black traces) and α -syn-PFF (cyan traces) animals at 12 weeks from injection. Scale bar 100 pA, 20 ms. Time-course graphs showing the mean EPSC amplitude, as a percentage of the baseline, of SPNs recorded before and for 20 min after an HFS (LTD protocol) in both sham and α -syn-PFF rats at 12 weeks post-surgery. Note the restored LTD in α -syn-PFF rats treated with L-DOPA (naïve to L-DOPA: α -syn-PFF $n = 9$; L-DOPA: sham $n = 8$; α -syn-PFF $n = 8$), $**P < 0.01$, two-way ANOVA. (D) Representative superimposed evoked EPSCs recorded from an SPN before and 20 min after the HFS protocol in Mg^{2+} -free external solution in sham (black traces) and α -syn-PFF (cyan traces) animals at 12 weeks from injection. Scale bar = 100 pA, 20 ms. Time-course graphs show the mean EPSC amplitude, as percentage of the baseline, of SPNs recorded before and for 20 min after the HFS (LTP protocol) in both L-DOPA-treated sham and α -syn-PFF rats at 12 weeks post-surgery. Note that, after the L-DOPA treatment, the impaired LTP observed in SPNs of α -syn-PFF rats at 12 weeks post-surgery was completely restored (naïve to L-DOPA: α -syn-PFF $n = 9$; L-DOPA: sham $n = 7$; α -syn-PFF $n = 11$, $***P < 0.001$, two-way ANOVA). (E) Representative traces of sEPSCs of SPNs of sham and α -syn-PFF rats at 12 weeks post-injection in the absence (left) or presence (right) of L-DOPA treatment. Scale bar = 20 pA, 1 s. Graphs of the sEPSC mean amplitude (left) and frequency (right) of SPNs recorded from sham and α -syn-PFF rats at 12 weeks post-injection in the presence or in the absence of L-DOPA treatment. Note that the increase of sEPSC frequency in α -syn-PFF rats is completely reverted by L-DOPA treatment (naïve to L-DOPA: sham $n = 11$; α -syn-PFF $n = 28$. L-DOPA: sham $n = 9$; α -syn-PFF $n = 10$), $**P < 0.01$, Student's *t*-test.

α -syn in Parkinson's disease pathology has been investigated in animal models that mirror the dopaminergic neuronal loss and widespread and progressive formation of α -syn aggregates in different areas of the brain. These models constitute a valuable tool for understanding the synaptic and molecular mechanisms of Parkinson's disease, possibly favouring the design of novel disease-modifying therapies.^{6,19,33} Among these models, the use of intrastriatal injection of α -syn-PFFs mimics various features of Parkinson's disease pathology in rodents, triggering Lewy body-like inclusions formation and spreading in brain regions directly interconnected with the injection site.^{6,19,20,33} This observation has suggested that there is an inter-neuronal transmission of the α -syn pathology.³ Taking the opportunity to use this progressive model, we have shown that some critical functional alterations occur at 6 and 12 weeks after the injection—long before complete neuronal degeneration.

We found phosphorylated α -syn in the SNpc as early as 6 weeks after the striatal injection, suggesting that this protein travels in a retrograde manner through the dopaminergic nigral axons in a very early phase of the process. Significant loss of dopaminergic terminals in the striatum was found at 6 and 12 weeks post-injection and this loss was associated with the reduced release of endogenous DA, indicating a precocious striatal dopaminergic dysfunction.

Specific motor and behavioural alterations occurred early in the model. In fact, the grid test revealed a motor impairment in rats 12 weeks after α -syn-PFF-injection compared with the control group. Indeed, this group of rats spent more time reaching the top of the grid and displayed hypokinesia during the task. Our observations are in line with clinical findings showing that relatively subtle deterioration of the motor system likely occurs well before the patient meets the established motor criteria for a clinical diagnosis of Parkinson's disease.³⁴ In fact, powerful compensatory mechanisms mask these clinical symptoms and make them difficult to identify and evaluate in the earliest stages of the illness.

Interestingly, behavioural alterations observed in the open field were already present 6 weeks post-injection. The open field task evaluates general locomotor deficits but also anxiety-like behaviours by testing the propensity to explore.²⁵ In line with our preclinical findings, clinical studies found that anxiety is more common in patients with Parkinson's disease at the time of diagnosis compared with the general population.³⁵ Notably, in the open field test α -syn-PFF rats showed no motor impairments, in contrast with the deficits observed in the grid-walking task, probably because the open field task is less challenging than the grid-walking task.

The possibility that the firing properties of DA SNpc neurons are altered before diffuse α -syn aggregation is a crucial question to explain the observed motor and behavioural alterations. In fact, DA cells provide a wide innervation to the striatum and changes in their firing rate might disrupt the activity and the plasticity of the striatal network, causing both motor and non-motor symptoms of Parkinson's disease.³⁶ Here we report that the activity of DA SNpc neurons is precociously changed in a time-dependent manner. We found that the spontaneous firing rate of DA SNpc neurons was absent in a large proportion of the cells recorded at 6 weeks post-injection. Conversely, at 12 weeks post-injection, the firing rate of these neurons increased in comparison with the sham-operated rats. The loss of spontaneous firing discharge observed at 6 weeks post-injection was associated with an initial neuronal loss and a deficit in striatal DA release. This may lead to reduced DA output that cannot be fully compensated, resulting in motor impairments. In line with our observations, reduced firing of DA SNpc neurons measured *in vivo* by juxtacellular recording of neurochemically identified neurons was found in a genetic mouse model of

synucleinopathy. These changes in SNpc neuron firing activity were detected in the absence of aggregates, possibly indicating that these electrophysiological alterations precede and are not caused by aggregate formation.³⁷

The increased firing rate measured at 12 weeks post-injection might have different explanations. In fact, at this later time window, some DA SNpc neurons were already dead, as shown by our morphological counting of TH+ neurons in the SNpc, and the remaining cells were overacting to compensate for this deficit. A possible alternative and/or complementary explanation was provided by the observation that, in a mouse model overexpressing mutant α -syn (A53T-SNCA), firing frequencies of DA SNpc neurons increased, similarly to our findings at 12 weeks post-injection. This increase of the intrinsic pacemaker frequency was associated with a redox-dependent decrease of the activity of A-type $K_{v}4.3$ potassium channels. Thus, the authors have postulated an enhancement of 'stressful pacemaking' of DA SNpc neurons as a functional response to mutant- α -syn before the onset of a widespread neurodegeneration.³⁸ In our study, however, we confirmed the finding on current-driven firing discharge of DA SNpc neurons from α -syn-injected animals at 12 weeks, but no significant change in the other measured intrinsic properties was detected. The increased firing rate of SNpc neurons observed in α -syn-PFF-injected animals at 12 weeks post-injection was coupled to a reduction in striatal DA release at the same time point. This apparent discrepancy might be related to the reduced number and altered function of DA terminals in the striatum at the same time point.

Our findings are in line with previous studies showing a significant decrease in striatal DA concentrations and mild motor effects at 12 weeks post α -syn-PFF-injection.⁶ However, our model shows more aggressive features such as a significant loss of TH-positive SNpc neurons as early as 12 weeks post α -syn-PFF-injection. Moreover, we observed reduced striatal TH immunoreactivity at 6 weeks post α -syn-PFF-injection, while previous studies reported similar changes only after 24 weeks.⁶ These discrepancies are possibly related to different experimental protocols (time points and amounts of injected α -syn-PFFs) as well as the animal species (rats versus mice). In fact, studies investigating α -syn-PFF-injected rats reported a significant reduction in SNpc TH+ neurons at 8 weeks³⁹ and 16 weeks.¹⁹

Although α -syn is highly expressed in neurons, particularly in DA and glutamatergic neurons,⁴⁰ it is still unclear whether mutant α -syn causes functional alterations of specific neuronal populations in the midbrain.^{41,42} Thus, we characterized the cell-type-specific functional vulnerability in SNpc and SNpr neurons. In line with the hypothesis of the selective neuronal vulnerability to α -syn caused by 'stressful pacemaker activity',^{43–45} in GABAergic neurons of SNpr, we observed changes in firing rate neither at 6 nor 12 weeks, supporting the idea of a specific vulnerability of DA midbrain neurons to α -syn.

Activity-dependent modifications in synaptic efficacy, such as LTD and LTP, are key cellular substrates for motor control and procedural memory. Thus, alterations to these two forms of synaptic plasticity in the striatum in the very early phases after α -syn injection can explain the onset and the progression of motor and non-motor symptoms induced by the dysfunctional activity of DA SNpc neurons. In fact, both LTD and LTP are regulated by dopaminergic transmission from nigrostriatal terminals. Changes in glutamatergic corticostriatal and dopaminergic nigrostriatal neuronal excitability profoundly influence the threshold for the induction of synaptic plasticity, and changes in striatal synaptic transmission efficacy are supposed to play a role in the occurrence of Parkinson's disease symptoms.⁴⁶ In this study, we found that these two forms of striatal synaptic plasticity are precociously lost in a

time-dependent manner. In fact, while LTP was already blocked at 6 weeks post-injection, LTD was impaired only at 12 weeks, when significant DA loss occurred.

Concerning the early loss of striatal LTP, which is a NMDA receptor-dependent form of synaptic plasticity, we assume that an α -syn-induced dysfunctional activity of postsynaptic NMDA receptors plays a major role. In line with this hypothesis, we recently conducted an electrophysiological analysis of corticostriatal slices, showing that α -syn oligomers reduce GluN2A NMDA receptor-mediated synaptic currents in the SPNs of both direct and indirect pathways.¹⁷

Concerning the loss of LTD, observed at 12 weeks but not at 6 weeks, we hypothesized that a relevant role is exerted by the significant decrease of endogenous striatal DA observed at this time window. To test this hypothesis, we subchronically treated α -syn-injected animals with L-DOPA, a precursor of DA that is considered the major resource in the symptomatic treatment of Parkinson's disease.⁴⁷ According to our hypothesis, L-DOPA treatment was able to restore both striatal LTD and LTP as well as reverse the motor deficits observed in the grid test at 12 weeks post-injection, indicating that both motor dysfunctions and plastic abnormalities observed at this time window are caused by striatal DA denervation. Conversely, this treatment only partially restored LTP at 6 weeks, further supporting the idea that, in addition to reduced tonic DA levels, other factors are impaired at this very early phase.

At 12 weeks post-injection, we also observed an increase in spontaneous excitatory transmission, resulting in an augmented frequency but not amplitude of sEPSCs. This suggested that in these animals glutamatergic transmission was enhanced by a presynaptic mechanism. Interestingly, this abnormal excitatory activity was normalized by subchronic L-DOPA treatment, indicating that it was caused by the reduced modulatory action of endogenous DA on glutamate release, possibly via retrograde signalling.⁴⁸ Enhancement of glutamatergic transmission in α -syn-PFF rats might involve a time-dependent spreading of α -syn-PFF into cortical areas. Accordingly, in the cortical regions of α -syn-PFF rats, we found few p- α -syn-positive neurons at the 6-week time point and a larger proportion at 12 weeks post-injection. The localization of these neurons was mainly in layers IV and V of the cortex (Supplementary Fig. 1).

It has been shown that D2 DA receptor activation reduces excitatory transmission onto SPNs and that this form of inhibition requires CB1 receptor activation.⁴⁸ This inhibitory effect is also blocked by postsynaptic intracellular calcium chelation. These results demonstrate a role for retrograde endocannabinoid signalling in the inhibition of glutamate release at presynaptic terminals by the activation of postsynaptic striatal D2 receptors. In line with this view, it can be hypothesized that, in α -syn-PFF rats at 12 weeks post-injection, the observed reduced DA transmission caused a decrease in D2 receptor activation on SPNs and, in turn, reduced the release of endocannabinoids from these neurons, acting in a retrograde manner on glutamatergic terminals. The final result of this scenario would be an increase of spontaneous glutamatergic activity in α -syn-injected animals. The efficacy of L-DOPA treatment in restoring normal spontaneous glutamatergic activity supports this hypothesis. However, we do not exclude that α -syn-PFF might directly influence endogenous α -syn homeostasis in presynaptic terminals, also influencing calcium buffering and neurotransmitter release.

The picture emerging from the present data suggests that, in the early phases of the disease, α -syn causes functional changes, leading to a reduced signal to noise ratio. In fact, while relevant phasic and plastic changes required for motor learning, such as LTP and LTD, are abolished, non-essential background information, driven by glutamatergic overactivity, is abnormally enhanced.

Conclusions

We show here for the first time that early and time-dependent concomitant alterations to the firing discharge of DA nigral neurons and striatal DA release, as well as deficits in striatal synaptic plasticity, occur in association with behavioural and motor signs, clearly mimicking the early stages of Parkinson's disease. These abnormalities are evident, even when cell death in the SNpc is partial and in the presence of a modest reduction of striatal DA terminals in the striatum. Nevertheless, these conditions are sufficient to affect the threshold of striatal dopaminergic signals required for physiological synaptic function and normal motor activity. In line with this interpretation, we found that subchronic treatment with L-DOPA, a DA precursor replacing the endogenous levels of this transmitter, is sufficient to reverse most of these abnormalities.

In conclusion, the progressive features of this early model of Parkinson's disease allowed us to profile circuit-specific deficits in DA neurotransmission associated with precocious alterations in neuronal functions and with a mild motor phenotype. Findings obtained from the analysis of these early phases of the disease allow us to advance our knowledge of the neuronal substrates leading to changes in DA and non-DA transmission in distinct basal ganglia regions and specific neuronal subtypes that differ in disease susceptibility. Our study might also help in setting the scenario for the use of disease modifying therapies in the early phases of Parkinson's disease.⁴⁹

Acknowledgements

The authors thank Prof. F. Fallarino and Dr G. Manni, Section of Pharmacology, University of Perugia, for performing the endotoxin assay.

Funding

This work was supported by grants from the Fresco Parkinson Institute to New York University School of Medicine and The Marlene and Paolo Fresco Institute for Parkinson's and Movement Disorders, with support from Marlene and Paolo Fresco (to V.G., P.C., A.C.), from Ministero dell'Istruzione, dell'Università e della Ricerca (MIUR) - PRIN (Bando 2017, Prot. 2017ENN4FY, E.D., F.G., N.B.M., P.C.) and from Ministero della salute, "Ricerca Corrente". This study was partially supported by an NIH grant (NS045962 to P.C. in collaboration with Drs Papa and Traynelis of Emory University, Atlanta, GA). The authors thank Fondazione Roma and Regione Umbria for supporting the research.

Competing interests

The authors report no competing interests.

Supplementary material

Supplementary material is available at *Brain* online.

References

1. Spillantini MG, Goedert M. Synucleinopathies: Past, present and future. *Neuropathol Appl Neurobiol.* 2016;42(1):3–5.
2. Luk KC, Song C, O'Brien P, et al. Exogenous alpha-synuclein fibrils seed the formation of Lewy body-like intracellular inclusions in cultured cells. *Proc Natl Acad Sci U S A.* 2009;106(47):20051–20056.

3. Hijaz BA, Volpicelli-Daley LA. Initiation and propagation of alpha-synuclein aggregation in the nervous system. *Mol Neurodegener.* 2020;15(1):19.
4. Cremades N, Cohen SI, Deas E, et al. Direct observation of the interconversion of normal and toxic forms of alpha-synuclein. *Cell.* 2012;149(5):1048–1059.
5. Ghiglieri V, Calabrese V, Calabresi P. Alpha-synuclein: From early synaptic dysfunction to neurodegeneration. *Front Neurol.* 2018;9:295.
6. Luk KC, Kehm V, Carroll J, et al. Pathological alpha-synuclein transmission initiates Parkinson-like neurodegeneration in nontransgenic mice. *Science.* 2012;338(6109):949–953.
7. Gallegos S, Pacheco C, Peters C, Opazo CM, Aguayo LG. Features of alpha-synuclein that could explain the progression and irreversibility of Parkinson's disease. *Front Neurosci.* 2015;9:59.
8. Wong YC, Krainc D. Alpha-synuclein toxicity in neurodegeneration: Mechanism and therapeutic strategies. *Nat Med.* 2017;23(2):1–13.
9. Cox J, Witten IB. Striatal circuits for reward learning and decision-making. *Nat Rev Neurosci.* 2019;20(8):482–494.
10. Graybiel AM, Grafton ST. The striatum: Where skills and habits meet. *Cold Spring Harb Perspect Biol.* 2015;7(8):a021691.
11. Calabresi P, Picconi B, Tozzi A, Ghiglieri V, Di Filippo M. Direct and indirect pathways of basal ganglia: A critical reappraisal. *Nat Neurosci.* 2014;17(8):1022–1030.
12. Calabresi P, Gubellini P, Centonze D, et al. Dopamine and cAMP-regulated phosphoprotein 32 kDa controls both striatal long-term depression and long-term potentiation, opposing forms of synaptic plasticity. *J Neurosci.* 2000;20(22):8443–8451.
13. Greengard P. The neurobiology of slow synaptic transmission. *Science.* 2001;294(5544):1024–1030.
14. Shen W, Flajolet M, Greengard P, Surmeier DJ. Dichotomous dopaminergic control of striatal synaptic plasticity. *Science.* 2008;321(5890):848–851.
15. Calabresi P, Pisani A, Rothwell J, Ghiglieri V, Obeso JA, Picconi B. Hyperkinetic disorders and loss of synaptic downscaling. *Nat Neurosci.* 2016;19(7):868–875.
16. Giordano N, Iemolo A, Mancini M, et al. Motor learning and metaplasticity in striatal neurons: Relevance for Parkinson's disease. *Brain.* 2018;141(2):505–520.
17. Durante V, de Iure A, Loffredo V, et al. Alpha-synuclein targets GluN2A NMDA receptor subunit causing striatal synaptic dysfunction and visuospatial memory alteration. *Brain.* 2019;142(5):1365–1385.
18. Henderson MX, Cornblath EJ, Darwich A, et al. Spread of alpha-synuclein pathology through the brain connectome is modulated by selective vulnerability and predicted by network analysis. *Nat Neurosci.* 2019;22(8):1248–1257.
19. Patterson JR, Duffy MF, Kemp CJ, et al. Time course and magnitude of alpha-synuclein inclusion formation and nigrostriatal degeneration in the rat model of synucleinopathy triggered by intrastriatal alpha-synuclein preformed fibrils. *Neurobiol Dis.* 2019;130:104525.
20. Stoyka LE, Arrant AE, Thrasher DR, et al. Behavioral defects associated with amygdala and cortical dysfunction in mice with seeded alpha-synuclein inclusions. *Neurobiol Dis.* 2020;134:104708.
21. Kirik D, Rosenblad C, Bjorklund A. Characterization of behavioral and neurodegenerative changes following partial lesions of the nigrostriatal dopamine system induced by intrastriatal 6-hydroxydopamine in the rat. *Exp Neurol.* 1998;152(2):259–277.
22. Chao OY, Pum ME, Li JS, Huston JP. The grid-walking test: Assessment of sensorimotor deficits after moderate or severe dopamine depletion by 6-hydroxydopamine lesions in the dorsal striatum and medial forebrain bundle. *Neuroscience.* 2012;202:318–325.
23. Starkey ML, Barritt AW, Yip PK, et al. Assessing behavioural function following a pyramidotomy lesion of the corticospinal tract in adult mice. *Exp Neurol.* 2005;195(2):524–539.
24. Z'Graggen WJ, Metz GA, Kartje GL, Thallmair M, Schwab ME. Functional recovery and enhanced corticofugal plasticity after unilateral pyramidal tract lesion and blockade of myelin-associated neurite growth inhibitors in adult rats. *J Neurosci.* 1998;18(12):4744–4757.
25. Seibenhener ML, Wooten MC. Use of the open field maze to measure locomotor and anxiety-like behavior in mice. *J Vis Exp.* 2015;(96):e52434.
26. Ledonne A, Nobili A, Latagliata EC, et al. Neuregulin 1 signalling modulates mGluR1 function in mesencephalic dopaminergic neurons. *Mol Psychiatry.* 2015;20(8):959–973.
27. Ting JT, Lee BR, Chong P, et al. Preparation of acute brain slices using an optimized N-methyl-D-glucamine protective recovery method. *J Vis Exp.* 2018;132:53825.
28. Nobili A, Latagliata EC, Viscomi MT, et al. Dopamine neuronal loss contributes to memory and reward dysfunction in a model of Alzheimer's disease. *Nat Commun.* 2017;8:14727.
29. Rizzo FR, Federici M, Mercuri NB. 3,4-Methylenedioxymethamphetamine (MDMA) alters synaptic dopamine release in the dorsal striatum through nicotinic receptors and DAT inhibition. *Neuroscience.* 2018;377:69–76.
30. Paxinos GW, Watson C. *The rat brain stereotaxic coordinates.* 5th ed. Elsevier Academic Press; 2005.
31. Bamford NS, Wightman RM, Sulzer D. Dopamine's effects on corticostriatal synapses during reward-based behaviors. *Neuron.* 2018;97(3):494–510.
32. Goedert M, Jakes R, Spillantini MG. The synucleinopathies: twenty years on. *J Parkinsons Dis.* 2017;7(s1):S51–S69.
33. Koprach JB, Kalia LV, Brotchie JM. Animal models of alpha-synucleinopathy for Parkinson disease drug development. *Nat Rev Neurosci.* 2017;18(9):515–529.
34. Maetzler W, Hausdorff JM. Motor signs in the prodromal phase of Parkinson's disease. *Mov Disord.* 2012;27(5):627–633.
35. Weintraub D, Simuni T, Caspell-Garcia C, et al.; the Parkinson's Progression Markers Initiative. Cognitive performance and neuropsychiatric symptoms in early, untreated Parkinson's disease. *Mov Disord.* 2015;30(7):919–927.
36. Singh A, Mewes K, Gross RE, DeLong MR, Obeso JA, Papa SM. Human striatal recordings reveal abnormal discharge of projection neurons in Parkinson's disease. *Proc Natl Acad Sci U S A.* 2016;113(34):9629–9634.
37. Janezic S, Threlfell S, Dodson PD, et al. Deficits in dopaminergic transmission precede neuron loss and dysfunction in a new Parkinson model. *Proc Natl Acad Sci U S A.* 2013;110(42):E4016–E4025.
38. Subramaniam M, Althof D, Gispert S, et al. Mutant alpha-synuclein enhances firing frequencies in dopamine substantia nigra neurons by oxidative impairment of A-type potassium channels. *J Neurosci.* 2014;34(41):13586–13599.
39. Paumier KL, Luk KC, Manfredsson FP, et al. Intrastriatal injection of pre-formed mouse alpha-synuclein fibrils into rats triggers alpha-synuclein pathology and bilateral nigrostriatal degeneration. *Neurobiol Dis.* 2015;82:185–199.
40. Taguchi K, Watanabe Y, Tsujimura A, Tanaka M. Expression of alpha-synuclein is regulated in a neuronal cell type-dependent manner. *Anat Sci Int.* 2019;94(1):11–22.
41. Alegre-Abarrategui J, Brimblecombe KR, Roberts RF, et al. Selective vulnerability in alpha-synucleinopathies. *Acta Neuropathol.* 2019;138(5):681–704.
42. Goedert M, Spillantini MG, Del Tredici K, Braak H. 100 years of Lewy pathology. *Nat Rev Neurol.* 2013;9(1):13–24.